
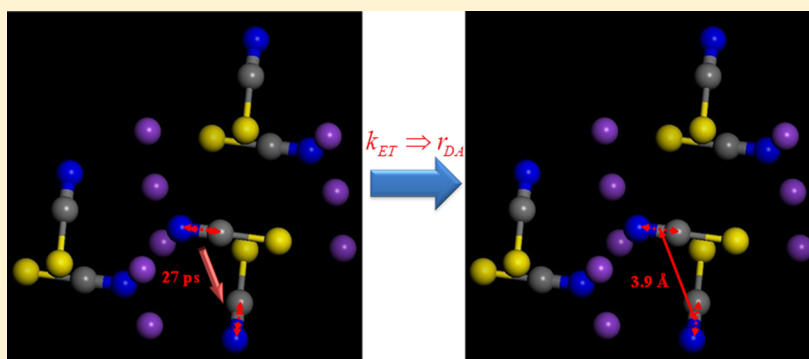


Molecular Distances Determined with Resonant Vibrational Energy Transfers

Hailong Chen,[†] Xiewen Wen,[†] Jiebo Li, and Junrong Zheng*

Department of Chemistry, Rice University, 6100 Main Street, Houston, Texas 77005-1892, United States

 Supporting Information



ABSTRACT: In general, intermolecular distances in condensed phases at the angstrom scale are difficult to measure. We were able to do so by using the vibrational energy transfer method, an ultrafast vibrational analogue of Förster resonance energy transfer. The distances among SCN^- anions in KSCN crystals and ion clusters of KSCN aqueous solutions were determined with the method. In the crystalline samples, the closest anion distance was determined to be $3.9 \pm 0.3 \text{ \AA}$, consistent with the XRD result. In the 1.8 and 1 M KSCN aqueous solutions, the anion distances in the ion clusters were determined to be $4.4 \pm 0.4 \text{ \AA}$. The clustered anion distances in aqueous solutions are very similar to the closest anion distance in the KSCN crystal but significantly shorter than the average anion distance (0.94–1.17 nm) in the aqueous solutions if ion clustering did not occur. The result suggests that ions in the strong electrolyte aqueous solutions can form clusters inside of which they have direct contact with each other.

1. INTRODUCTION

Short-ranged transient intermolecular interactions, for example, guest/host interactions, ion/ion interactions, and ion/molecule bindings, play significant roles in chemistry and biology. Electronic energy transfer methods, for example, Förster resonance energy transfer (FRET), are routinely applied to measure the distance between two molecules in many of these interactions.^{1,2} In these methods, chromophores that can transfer and accept energy in the visible and near-IR frequency range are required to attach to molecules. The chromophores are typically at the size of 1–2 nm or larger, which is not only much larger than many of the intermolecular distances but also can perturb the molecular interactions under investigation. To probe molecular distances at the angstrom scale, what is needed is an ultrafast vibrational analogue of FRET of which the chromophores are simple chemical bonds (1–2 Å).

Here, by measuring ultrafast vibrational energy transfers in model systems of KSCN (potassium thiocyanate) crystals and aqueous solutions, we demonstrate that angstrom molecular distances in condensed phases can be determined. In this paper, we first present anisotropy decay and vibrational energy exchange data to show that vibrational energy can transfer resonantly among SCN^- anions and nonresonantly from SCN^- to $\text{S}^{13}\text{C}^{15}\text{N}^-$ with much slower rates in KSCN/ $\text{KS}^{13}\text{C}^{15}\text{N}$ mixed

crystals. A kinetic model is then developed to quantitatively analyze the resonant energy transfer data to obtain the resonant energy transfer time between two adjacent anions in the crystals. To convert the energy transfer time into distance, an equation based on the dephasing mechanism and the time-dependent Schrödinger equation is derived to correlate the energy transfer time with the energy donor/acceptor coupling strength, which is quantitatively correlated to the donor/acceptor distance under the dipole/dipole interaction. On the basis of the energy transfer equation and the dipole/dipole interaction equation and the measured energy transfer time, the distance between the two adjacent anions is calculated. The calculated distance is then compared to the distance measured by XRD. Within experimental uncertainty, the two values are the same. The uncertainty introduced by the point dipole assumption used in the method is then calculated based on the monopole theory. It is found that the uncertainty is very small, only ~1.3%, mainly because the donor/acceptor distance is more than three times larger than the sizes of the donor/acceptor. After benchmarking the vibrational energy transfer

Received: January 17, 2014

Revised: March 17, 2014

Published: March 18, 2014

method with the crystalline sample, the method is used to determine the anion distance in the ion clusters of KSCN aqueous solutions. It is found that within experimental uncertainty, the anion distance in the clusters is the same as that in the crystal.

2. EXPERIMENTS AND METHODS

2.1. Laser System. A ps amplifier and a fs amplifier are synchronized with the same seed pulse. The ps amplifier pumps an OPA to produce ~ 0.8 ps (vary from 0.7–0.9 ps in different frequencies) mid-IR pulses with a bandwidth of $10\text{--}35\text{ cm}^{-1}$ in a tunable frequency range from 400 to 4000 cm^{-1} with an energy of $1\text{--}40\text{ }\mu\text{J/pulse}$ ($1\text{--}10\text{ }\mu\text{J/pulse}$ for $400\text{--}900\text{ cm}^{-1}$ and $>10\text{ }\mu\text{J/pulse}$ for higher frequencies) at 1 kHz. Light from the fs amplifier is used to generate a high-intensity mid-IR and terahertz supercontinuum pulse with a duration of <100 fs in the frequency range from <10 to $>3500\text{ cm}^{-1}$ at 1 kHz. In nonlinear IR experiments, the ps IR pulse is the excitation beam (the excitation power is adjusted based on need, and the interaction spot varies from 100 to $500\text{ }\mu\text{m}$). The supercontinuum pulse is the probe beam that is frequency-resolved by a spectrograph (the resolution is $1\text{--}3\text{ cm}^{-1}$, dependent on the frequency), yielding the detection axis of a 2D IR spectrum. Two polarizers are added into the detection beam path to selectively measure the parallel or perpendicular polarized signal relative to the excitation beam.

2.2. Vibrational Energy Transfer Measurements. Vibrational lifetimes are obtained from the rotation-free $1\text{--}2$ transition signal $P_{\text{life}} = P_{\parallel} + 2 \times P_{\perp}$, where P_{\parallel} and P_{\perp} are parallel and perpendicular data, respectively. The time-dependent anisotropy values are acquired from $r(t) = (P_{\parallel} - P_{\perp}) / (P_{\parallel} + 2 \times P_{\perp})$, with the definition of time zero being a pump–probe delay of zero. The resonant energy transfer rate constants and the molecular rotational time constants in the samples are obtained from the anisotropy measurements. The isotropic distribution of a sample within the laser focus spot is tested by measuring the initial anisotropy values of the sample at different angles relative to the polarization of the excitation beam.

The nonresonant vibrational energy transfers among the regular KSCN and isotope-labeled $\text{KS}^{13}\text{C}^{15}\text{N}$ and KS^{13}CN are measured with the vibrational energy exchange method.^{3–5} In the measurements, the donor vibrational mode, for example, the CN (nitrile) stretch of KSCN is excited to its first vibrational excited state with an ultrafast IR pulse. The time-dependent decay of this CN first excited-state population is then monitored in real time with another laser pulse. Simultaneously, the first excited-state population of the acceptor mode, for example, the $^{13}\text{C}^{15}\text{N}$ stretch of $\text{KS}^{13}\text{C}^{15}\text{N}$, is also monitored in real time right after the donor is excited to its first excited state. Simultaneous analyses of the decay of the donor first excited-state population and the growth and decay of the acceptor first excited-state population according to the energy transfer kinetic model^{3–5} quantitatively yield the vibrational energy transfer rate constant from the donor to the acceptor. Here, the vibrational mode that is excited by the laser is defined as the “donor”. The mode that is not excited by laser but can accept energy from the donor is defined as the “acceptor”. Experimentally, we can change the frequencies of the laser to selectively excite either the CN or $^{13}\text{C}^{15}\text{N}$ stretch so that both forward and backward energy transfers between these two stretches can be determined. The resonant energy transfers among the thiocyanate anions are measured with the resonant energy transfer induced anisotropy decay method.^{4,6} In these

measurements, the nitrile stretch of one anion, for example, SCN^- , is excited to its first excited state. The decay of the anisotropy value of this vibrational excitation signal is then monitored in real time. Simultaneous analyses on the anisotropy decays in samples with different mixed $\text{KSCN}/\text{KS}^{13}\text{C}^{15}\text{N}$ ratios quantitatively yield both the resonant energy transfer rate constant and the rotational time constant of the anion.

2.3. Samples. Unless specified, chemicals were purchased from Sigma–Aldrich and used without further purification. $\text{KS}^{13}\text{C}^{15}\text{N}$ was purchased from Cambridge Isotope Laboratory. The samples were thin films of polycrystalline $\text{KSCN}/\text{KS}^{13}\text{C}^{15}\text{N}$ mixed crystals with different molar ratios blended with ~ 50 wt % PMMA. The thickness of the sample is estimated to be a few hundred nm based on the CN stretch optical density. An optical image of a sample is provided in Figure S1 in the Supporting Information (SI). The function of PMMA was to suppress scattered light. The samples were placed in a vacuum chamber during measurements. There are four reasons to use KSCN and $\text{KS}^{13}\text{C}^{15}\text{N}$ and KS^{13}CN as model systems: (1) the vibrational lifetimes of the nitrile stretches are relatively long (longer than 30 ps in D_2O solutions and even longer in the crystals as included in the SI);⁴ (2) the transition dipole moments of the nitrile stretches are relatively large ($0.3\text{--}0.4\text{ D}$);⁴ (3) the distance between any two anions in the KSCN crystal is well-characterized with XRD and neutron scattering, which can be used to benchmark the distance determined by the vibrational energy transfer method;⁷ and (4) the phonon dispersion in the KSCN crystal was well-characterized before.^{8,9}

The purpose of using different-isotope-labeled thiocyanate anion mixed samples, for example, a $\text{KSCN}/\text{KS}^{13}\text{C}^{15}\text{N}$ mixed crystal with different molar ratios, is 2-fold, (1) to shift the vibrational frequency of the nitrile stretch as the vibrational frequency of the CN stretch is different from that of the $^{13}\text{C}^{15}\text{N}$ stretch and (2) to change the number of resonant energy transfer acceptors in the samples without changing the crystalline structure or ion cluster structure because the isotope labeling has negligible effects on the intermolecular interaction between two thiocyanate anions that determines their distance and relative orientation.¹⁰

3. RESULTS AND DISCUSSION

3.1. Vibrational Energy Transferring among SCN^- Anions in the KSCN Crystal. Figure 1 displays the time-dependent normalized anisotropy values of the nitrile stretch (1st excited state) excitation of thiocyanate anion in two samples, (A) a 2% $\text{KS}^{13}\text{C}^{15}\text{N}$ in 98% KSCN ($\text{KS}^{12}\text{C}^{14}\text{N}$) mixed crystal (black) where $\text{S}^{13}\text{C}^{15}\text{N}^-$ is excited and (B) a pure KSCN crystal (red) where SCN^- is excited. In sample A, the anisotropy decays relatively slowly, with a single-exponential time constant of ~ 12 ps, and its residual anisotropy value at the delay time of 40 ps is $\sim 50\%$ of its initial value. In sample B, the anisotropy decays much faster, with a time constant ~ 1.8 ps. Its residual anisotropy value at 40 ps is only $\sim 12\%$ of the initial value. In general, the anisotropy decays have two possible molecular origins, (1) molecular reorientational motions and (2) energy transfers to molecules with different orientations. Both contribute to the orientational randomization of vibrational excitations and lead to the decay of signal anisotropy.¹¹ In the two samples, the crystalline structures and molecular interaction strengths are expected to be hardly changed by the isotope labeling with ^{13}C and ^{15}N on the anions because the

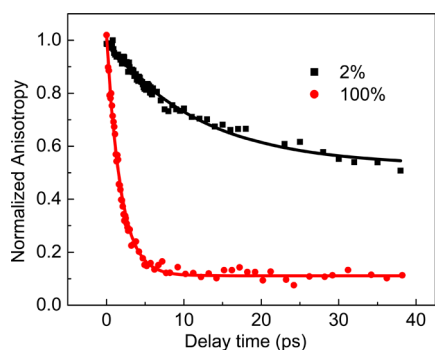


Figure 1. Time-dependent normalized anisotropy values of the nitrile stretch (1st excited state) excitation of the thiocyanate anion in two samples at room temperature: (A) a 2% $\text{KS}^{13}\text{C}^{15}\text{N}$ in 98% KSCN mixed crystal (black) where $\text{S}^{13}\text{C}^{15}\text{N}^-$ is excited and (B) a pure KSCN crystal (red) where SCN^- is excited. The decay of anisotropy indicates how fast the orientation of the vibrational excitation randomizes. Dots are data. Curves are single-exponential fits with time constants of 12 (sample A) and 1.8 ps (sample B). The 2 and 100% labels in represent the percentage of the resonant energy acceptors in the samples.

electronic structures of the atoms are expected to be little affected by the small changes of the atomic mass of the isotopes¹⁰ and thus are essentially the same. Therefore, the anisotropy decays caused by molecular reorientational motions (wobbling) are very similar for the two samples. The observed large difference in anisotropy decay rate can only be caused by different energy transfer dynamics in the two samples.

In sample A, most of the neighbors of any excited $\text{S}^{13}\text{C}^{15}\text{N}^-$ are SCN^- ($\text{S}^{12}\text{C}^{14}\text{N}^-$). In sample B, all neighbors of the excited

SCN^- are also SCN^- . The nitrile stretch energy transfer rate from a $\text{S}^{13}\text{C}^{15}\text{N}^-$ to a SCN^- is very different from the rate for energy transfer from one SCN^- to another SCN^- . As measured, the 0–1 transition frequency of the nitrile stretch of $\text{S}^{13}\text{C}^{15}\text{N}^-$ is 1975 cm^{-1} , 75 cm^{-1} smaller than that (2050 cm^{-1}) of SCN^- . The vibrational energy exchange rate between SCN^- and $\text{S}^{13}\text{C}^{15}\text{N}^-$ was directly measured using the vibrational energy exchange method.⁴ From the 2D IR spectra shown in Figure 2, our vibrational energy exchange kinetic model,^{3,4} and the principle of detailed balance, which requires that at equilibrium the populations at two energy levels fulfill the Boltzmann distribution, the energy transfer time constant ($1/k_{\text{S}^{13}\text{C}^{15}\text{N}^- \rightarrow \text{SCN}^-}$) from $\text{S}^{13}\text{C}^{15}\text{N}^-$ (1975 cm^{-1}) to SCN^- (2050 cm^{-1}) is determined to be $140 \pm 7\text{ ps}$ in a $\text{KSCN/KS}^{13}\text{C}^{15}\text{N} = 1/1$ mixed crystal. Details of this analysis are provided in the SI. This result indicates that the anisotropy decay caused by the two-stepped energy transfer from one $\text{S}^{13}\text{C}^{15}\text{N}^-$ to one SCN^- and from this SCN^- to another $\text{S}^{13}\text{C}^{15}\text{N}^-$ must be slower than 236 ps (the sum of the energy transfer times of the two-step energy transfer processes: $140 + 140 \times e^{-75/200} = 236\text{ ps}$) in sample A. This value is significantly longer than the measured anisotropy decay constant of 12 ps in sample A, indicating that the contribution of nonresonant energy exchanges between $\text{S}^{13}\text{C}^{15}\text{N}^-$ and SCN^- to the experimentally measured total anisotropy decay in sample A is negligible on this time scale. The contribution from resonant energy transfers among $\text{S}^{13}\text{C}^{15}\text{N}^-$ is also very small because the number of resonant energy acceptors in sample A is only 1/50 of that in sample B, which implies that the resonant energy transfer time in sample A should not be faster than 90 ps ($1.8 \times 50 = 90\text{ ps}$) as the total energy transfer rate is linearly proportional to the total number

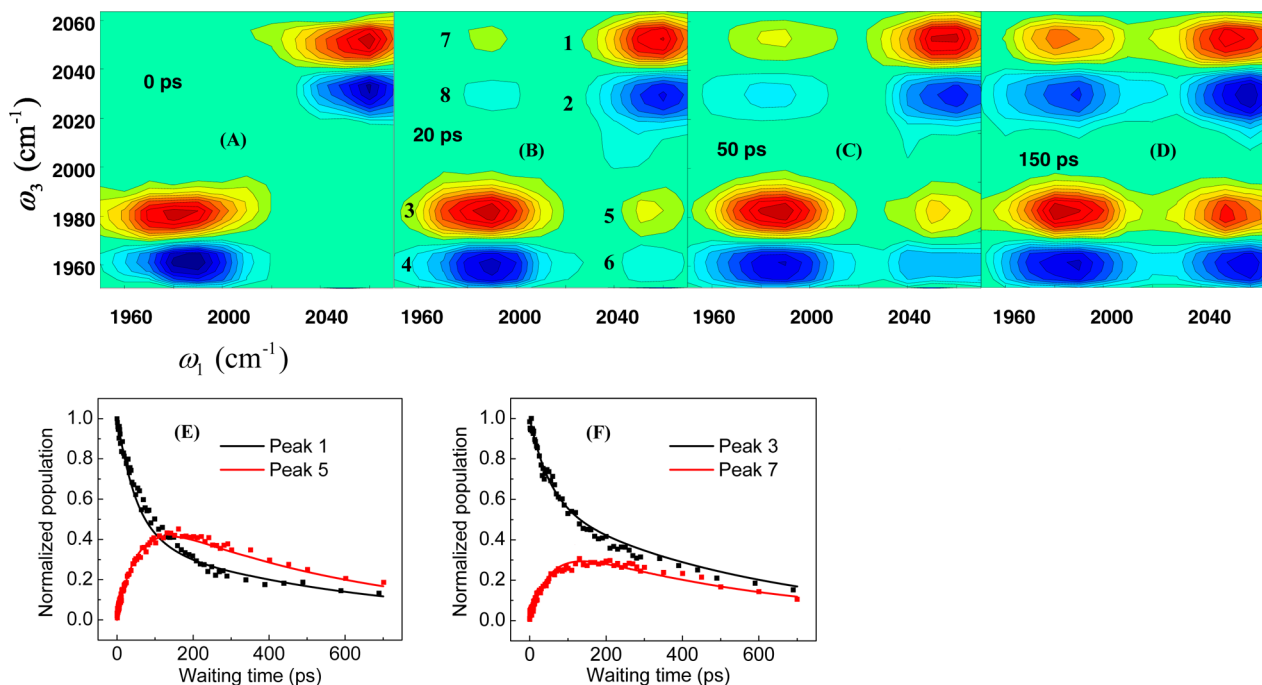


Figure 2. (A–D) Delay-time-dependent vibrational energy exchange 2D IR spectra of a $\text{KSCN/KS}^{13}\text{C}^{15}\text{N} = 1/1$ mixed crystal at room temperature. The growth of cross peaks 5–8 indicates how fast the vibrational energy exchange proceeds between SCN^- and $\text{S}^{13}\text{C}^{15}\text{N}^-$. (E,F) Delay-time-dependent normalized intensities of peaks 1, 3, 5, and 7. Dots are experimental data, and curves are calculations based on the energy exchange kinetic model and experimentally measured vibrational lifetimes. Peaks 1 and 2 are the 0–1 and 1–2 transitions of the CN stretch, respectively, generated from direct laser excitation. Peaks 3 and 4 are the 0–1 and 1–2 transitions of the $^{13}\text{C}^{15}\text{N}$ stretch, respectively, generated from direct laser excitation. Peaks 5 and 6 are the 0–1 and 1–2 transitions of the $^{13}\text{C}^{15}\text{N}$ stretch, generated from the energy transfer process from CN to $^{13}\text{C}^{15}\text{N}$. Peaks 7 and 8 are the 0–1 and 1–2 transitions of the CN stretch, generated from the energy transfer process from $^{13}\text{C}^{15}\text{N}$ to CN.

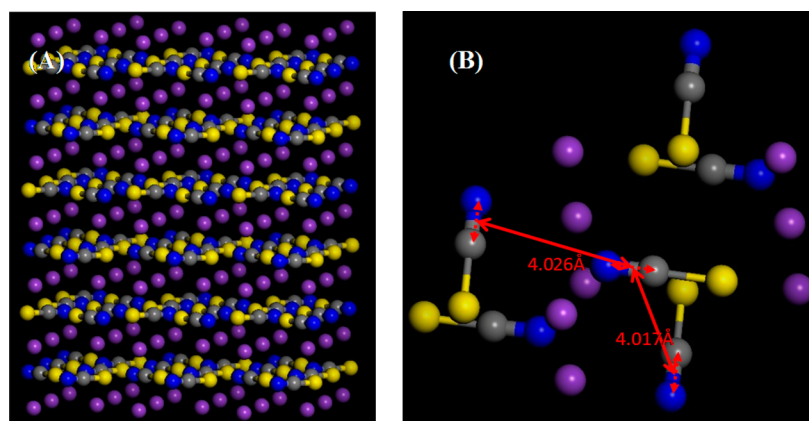


Figure 3. Crystalline structure of the KSCN crystal at room temperature. K is represented by purple balls, yellow balls for S, gray balls for C, and blue balls for N.

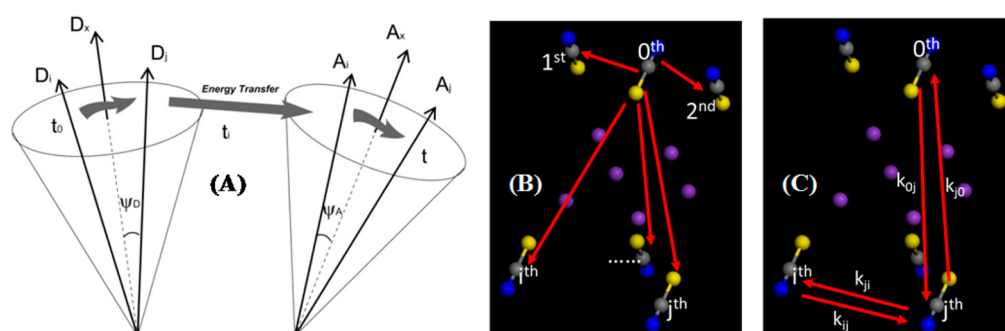


Figure 4. (A) Illustration of molecular wobbling and vibrational energy transfer from the donor (D) to acceptor (A). ψ_D and ψ_A are the wobbling angles of D and A, respectively. (B,C) Energy exchange process.

of available resonant energy acceptors. Therefore, the observed initial anisotropy decay with a time constant of 12 ps in sample A is mainly from the molecular wobbling motions inside of the crystal plus a small contribution from vibrational energy transfers. The observed anisotropy decay with a time constant of 1.8 ps in sample B is mainly caused by resonant energy transfers among SCN^- anions plus a small contribution from molecular wobbling.

In contrast with the resonant vibrational energy transfer from one donor to randomly orientated acceptors in liquids, which causes anisotropy to decay to zero,^{4,6} the anisotropy does not decay to zero in the KSCN crystalline samples because the molecular orientations inside of the crystal are roughly confined to planes because the rotational motion (wobbling) of SCN^- is hindered, and therefore, the orientations are not random. As shown in the crystalline structure in Figure 3,⁷ two adjacent anions in the KSCN crystal are either perpendicular or parallel to each other. The two shortest distances between the CN bond central points, 4.017 and 4.026 Å,⁷ are both between perpendicular anion pairs (Figure 3B). In both cases, the connection lines between the central points of the CN bonds are not perpendicular to the transition dipole moment direction of either CN stretch, which is along the CN bond direction. This structure allows vibrational energy to transfer from one anion to another perpendicular anion through the second term of the dipole–dipole interaction ($\mu \cdot \mu / r^3 - 3(\mu \cdot r)(\mu \cdot r) / r^5$).

3.2. Transfer Energy Time from One SCN^- to One Adjacent Perpendicular SCN^- 4.017 Å Away: 27 ± 3 ps. To extract the resonant energy transfer rate constant between two CN stretches from the anisotropy measurements, we

developed a kinetic model that accounts for both molecular wobbling and resonant energy transfer. As illustrated in Figure 4A, in the crystal at room temperature, the wobbling motions and vibrational energy transfers of SCN^- anions occur simultaneously with different time constants. Experimentally, by adjusting the laser intensity and spot size, only 0.1–0.5% of the anions are excited by the laser within the laser focus spot. In other words, for one energy donor, on average, there are about 200–1000 acceptors available to which energy transfer is not completely negligible. Therefore, in the kinetic model, the model sample is a small KSCN crystal with a finite number of anions. Crystals with three different sizes are used in the analyses, (1) with 108 anions (~three layers), (2) with 500 anions (~five layers), and (3) with 1372 anions (~seven layers). In each small crystal, only the central SCN^- anion is the original energy donor excited by the laser, which is called the zeroth molecule (Figure 4B). Other anions are initial energy acceptors, which are called the first, second, ..., *i*th, and *j*th molecules. The vibrational energy can exchange among all anions, as illustrated in Figure 4C. Besides transferring energy, the anions can also wobble with a time constant τ_c . Both dynamic processes cause the anisotropy of the CN stretch excitation to decay. Because the wobbling motion is a hindered rotation and the orientations of the crystallites in the powder sample are random, there will be a residual anisotropy A_∞ at the infinitely long delay time.

On the basis of the physical picture described above, the CN stretch excitation probabilities are related to the experimentally measured anisotropy $r(t)$ by

$$r(t) = p_0(t) \cdot r_0(t) + p_{\parallel}(t) \cdot r_{\parallel}(t) + p_{\perp}(t) \cdot r_{\perp}(t) \quad (1)$$

where $p_0(t)$, $p_{\parallel}(t)$, and $p_{\perp}(t)$ are the vibrational excitation probabilities of the zeroth molecule, all other anions parallel to the zeroth anion, and all anions perpendicular to the zeroth anion, respectively, which are determined by the energy transfer rate constants k_{ij} between any two anions i and j . $r_0(t)$, $r_{\parallel}(t)$, and $r_{\perp}(t)$ are the anisotropy values of the zeroth SCN^- , all other SCN^- parallel to the zeroth SCN^- , and all SCN^- perpendicular to the zeroth SCN^- , respectively (detailed derivations are provided in the SI).^{12,13}

$$\frac{r_0(t)}{r(0)} = \left[(1 - A_{\infty}) \exp\left(\frac{-t}{\tau_c}\right) + A_{\infty} \right] \quad (2)$$

$$\frac{r_{\parallel}(t)}{r(0)} = A_{\infty} \left[(1 - A_{\infty}) \exp\left(\frac{-t}{\tau_c}\right) + A_{\infty} \right] \quad (3)$$

$$\frac{r_{\perp}(t)}{r(0)} = -\left(\frac{1}{2}\right) A_{\infty} \left[(1 - A_{\infty}) \exp\left(\frac{-t}{\tau_c}\right) + A_{\infty} \right] \quad (4)$$

in which τ_c is the reorientational time constant and A_{∞} is the residue reorientation anisotropy at the infinitely long delay time.

In using eq 1 to analyze the resonant vibrational energy transfer rates in the KSCN mixed crystals, only three parameters are unknown, the residue anisotropy A_{∞} , the reorientational time constant τ_c , and the energy transfer rate constant ($1/k_{01}$) between the two perpendicular anions with the shortest CN distance of 4.017 Å (Figure 3B). The rate constants between any other two anions can be determined based on $1/k_{01}$ and eqs 9–11 described in a later paragraph. Experimentally, by varying the ratio of KSCN/ $\text{KS}^{13}\text{C}^{15}\text{N}$, the values of k_{01} (and therefore the total energy transfer rate constant k) and τ_c can be respectively constrained into a very small range, for example, as discussed above, the anisotropy decay time constant in the $\text{KS}^{13}\text{C}^{15}\text{N}/\text{KSCN} = 2/98$ sample must be very close to τ_c (10 ps) and that in the pure KSCN crystal must be close to $1/k$ (1.8 ps). Calculations with parameters $A_{\infty} = 0.70 \pm 0.06$, $1/k_{01} = 27 \pm 3$ ps, and $\tau_c = 10.0 \pm 1$ ps simultaneously fit the experimental results of five samples (donor/acceptor = 2/98, 14/86, 35/65, 65/35, and 100/0) very well, as displayed in Figure 5. (We also calculated the time-dependent anisotropies by considering the convolution of the signal with the instrument response function and found no difference between the deconvoluted and undeconvoluted results. The results are provided in the SI.) We also found that analyses on crystals with different numbers of anions (108, 500, and 1372) give essentially the same rate constants. The difference is within 2%. This is because in the dipole/dipole interaction or higher-order interactions involved in energy transfers, the anisotropy decay is mainly the result of the energy transfers among the closest anions. All of the energy transfer time constants $1/k_{ij}$ determined with a model crystal with 500 SCN^- anions are listed in Table S2 in the SI.

3.3. Resonant Vibrational Energy Transfer Rate Determined by the Coupling Strength and Dephasing Time. The energy transfer rate constant can be theoretically correlated to the D/A distance. For the energy transfer system, the system state can be expressed as

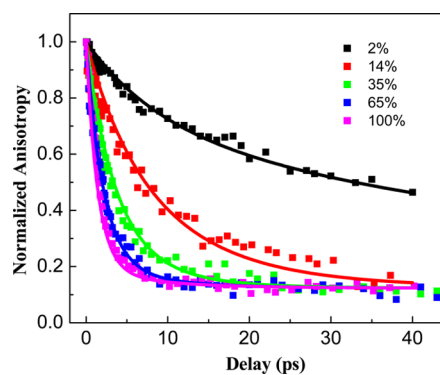


Figure 5. Time-dependent anisotropies of KSCN/ $\text{KS}^{13}\text{C}^{15}\text{N}$ mixed crystals with different molar percentages of resonant energy donor species at room temperature. Dots are experimental results, and curves are calculations. Each percentage value in the figure represents the percentage of the resonant energy acceptor in each sample.

$$|\psi\rangle = c_1(t)e^{-i\omega_D t}|D=1, A=0\rangle + c_2(t)e^{-i\omega_A t}|D=0, A=1\rangle \quad (5)$$

where ω_D and ω_A are the 0–1 transition frequency of the donor and the acceptor, respectively. $|D=1, A=0\rangle$ is the donor state where the donor (D) is at the first excited state and the acceptor (A) is at the ground state, and $|D=0, A=1\rangle$ is the acceptor state where the donor (D) is at the ground state and the acceptor (A) is at the first excited state. $c_1(t)$ and $c_2(t)$ are the coefficients of these two states, with $|c_1(t)|^2 + |c_2(t)|^2 \equiv 1$. Substituting eq 5 into the time-dependent Schrödinger equation, we can obtain using the rotating wave approximation

$$c_1(t) = e^{(1/2)i\Delta\omega t} \left[\cos\left[\frac{t}{2}\sqrt{(\Delta\omega)^2 + 4\beta^2}\right] - i \frac{\Delta\omega \sin\left[\frac{t}{2}\sqrt{(\Delta\omega)^2 + 4\beta^2}\right]}{\sqrt{(\Delta\omega)^2 + 4\beta^2}} \right] \quad (6)$$

$$c_2(t) = \frac{2\beta e^{-(1/2)i\Delta\omega t} \sin\left(\frac{t}{2}\sqrt{(\Delta\omega)^2 + 4\beta^2}\right)}{\sqrt{(\Delta\omega)^2 + 4\beta^2}} \quad (7)$$

where $\Delta\omega = \omega_A - \omega_D$ and $\beta = (\langle\langle D=1, A=0|H|D=0, A=1\rangle\rangle/\hbar) = (\langle\langle D=0, A=1|H|D=1, A=0\rangle\rangle/\hbar)$, where H is the system Hamiltonian. For an ensemble of D/A pairs with each pair evolving with eqs 6 and 7, the coherence is proposed to be terminated by an abrupt dephasing event at time t_c so that the D/A pair will stay in the acceptor state with probability $|c_2(t_c)|^2$. For the ensemble, the average probability on the acceptor state is $P = \int_0^\infty |c_2(t_c)|^2 p(t_c) dt_c$, where $p(t_c) = \tau^{-1}e^{-t_c/\tau}$ is the probability of dephasing at time t_c with $\int_0^\infty p(t_c) dt_c = 1$.¹⁴ τ is the dephasing time during which the dephasing probability is equal for any time interval, and it can be determined from the energy-mismatch ($\Delta\omega$)-dependent energy transfer experiments (details are provided in the SI). The population growth rate constant of the acceptor, is therefore

$$k_p = \frac{P}{\tau} = 2\beta^2 \frac{\frac{1}{\tau}}{(\Delta\omega)^2 + 4\beta^2 + \tau^{-2}} \quad (8)$$

Because the population growth rate constant is the sum of the energy transfer rate constant from the donor to the acceptor and acceptor to donor (the derivation is provided in the SI) and the rate of acceptor to donor is determined by detailed balance, the observable transfer rate constant from the donor to the acceptor is

$$k_{DA} = \frac{k_p}{1 + e^{\Delta\omega/kT}} = \frac{2}{1 + e^{\Delta\omega/kT}} \beta^2 \frac{\frac{1}{\tau}}{(\Delta\omega)^2 + 4\beta^2 + \tau^{-2}} \quad (9)$$

Equation 9 is for the weak coupling limit. In other words, it is not suitable to describe coherent energy transfers. If the coupling is weak, $(2\beta)^2 \ll \tau^{-2}$ (τ^{-2} is in energy units), and k_{DA} is proportional to β^2 , which is proportional to r_{DA}^{-6} under the transition–dipole/transition–dipole interaction mechanism²

$$\beta^2 = \frac{1}{n^4} \frac{\mu_D^2 \mu_A^2}{(4\pi\epsilon_0)^2} \frac{\kappa^2}{r_{DA}^6} \quad (10)$$

where n is the refractive index. The local field correction factor for the refractive index² is not used in the analysis because all D/A pairs in the studied systems are separated by other ions (even the closest pair has K^+ cations between them). ϵ_0 is the vacuum permittivity. μ_D and μ_A are the transition dipole moments of the donor and acceptor respectively. r_{DA} is the distance between the donor and acceptor, which is defined as the distance between the CN center points of two SCN^- anions in the crystals. κ is the orientation factor defined in eq 11

$$\begin{aligned} \langle \kappa^2 \rangle &= \kappa_0^2 \langle d_D \rangle \langle d_A \rangle + \frac{1}{3} (1 - \langle d_D \rangle) + \frac{1}{3} (1 - \langle d_A \rangle) \\ &+ \cos^2 \Theta_D \langle d_D \rangle (1 - \langle d_A \rangle) + \cos^2 \Theta_A \langle d_A \rangle (1 - \langle d_D \rangle) \end{aligned} \quad (11)$$

where $\kappa_0^2 = (\sin \Theta_D \sin \Theta_A \cos \Phi - 2 \cos \Theta_D \cos \Theta_A)^2$, Θ_D , Θ_A , and Φ are the angles defined in Figure S2 (SI), and $\langle d_D \rangle = \langle d_A \rangle = (A_\infty)^{1/2}$. Equation 11 is averaged over all wobbling angles.¹⁵ (The derivation is provided in the SI.)

Equations 9–11 thus connect the resonant energy transfer rate constant k_{DA} with the D/A distance r_{DA} . All parameters in the equations are experimentally accessible.

3.4. Energy Donor/Acceptor Distance Determined to Be 3.9 ± 0.3 Å from the Transfer Time Constant. From both 1D IR and 2D IR, the transition dipole moment of the CN stretch of SCN^- in KSCN crystals was determined to be $\mu_D = \mu_A = 0.31 \pm 0.03D$. From eq 11 and XRD data and the determined $A_\infty = 0.70 \pm 0.06$, the orientation factor between the two closest SCN^- anions is determined to be $(\langle \kappa^2 \rangle)^{1/2} = 0.378$. The refractive index is $n = 1.5 \pm 0.05$.¹⁶ The dephasing time is $\tau = 0.66$ ps (8 cm^{-1} , $\tau = (1/2\pi)(100/8 \times 3)$ ps). On the basis of these experimental parameters and the energy transfer time constant $1/k_{DA} = 27 \pm 3$ ps, the calculation from eqs 9–11 gives the energy donor/acceptor distance (taken as the distance between the CN central points of the donor and acceptor because the CN stretch is mainly localized within the CN bond according to DFT calculations) $r_{DA} = 3.9 \pm 0.3$ Å. This value is very close to the XRD-determined distance of 4.017 Å.

3.5. Minor Corrections from High-Order Interactions.

In calculating electronic energy transfers, if the D/A distance is comparable to the sizes of chromophores, the assumption of the point dipole in the dipole/dipole interaction can cause a significant uncertainty.¹⁷ Corrections from higher-order interactions are needed to obtain more precise results. An efficient

way to solve this problem is the monopole/monopole interaction, which counts for the charge interactions among individual atoms.¹⁷ In the KSCN crystals studied in this work, the two closest D/A distances are about 4 Å, which is larger but not significantly larger than the CN bond length (1.1–1.2 Å). It is conceivable that higher-order interactions could matter. To address this issue, we calculated the coupling constant from the monopole/monopole interaction and found that it is only 1.3% different from that calculated from the dipole/dipole interaction, which is the first-order approximation of the monopole/monopole interaction. The calculations show that the higher-order interactions play minor roles in the systems studied. Detailed calculations are provided in the SI.

3.6. Anion Distances in Ion Clusters in KSCN Aqueous Solutions: $r_{DA} = 4.4 \pm 0.4$ Å. Using eqs 9–11 to determine angstrom distances from vibrational energy transfer rate constants is not limited only to solid samples. The approach is also applicable for liquids. We have determined that in the 1 and 1.8 M KSCN aqueous solutions, more than 25% of the ions form clusters, and on average, the clusters contain three (1 M) and four (1.8 M) SCN^- anions.⁴ The resonant one-donor-to-one-acceptor energy transfer time constants were determined to be 15 (1 M) and 18 ps (1.8 M), respectively (Figures S6 and S7 in the SI), based on the method introduced previously.⁴ The transfer time in the 1.8 M solution seems slightly slower than that in the 1 M solution, but the difference is within the experimental uncertainty. On the basis of these energy transfer time constants and eqs 9–11, the distances between two SCN^- anions in the clusters in the two solutions are determined to be $r_{DA} = 4.4 \pm 0.4$ Å. Calculation details and experimental data are provided in the SI. The determined clustered anion distances are significantly shorter than the average anion distance (~ 1 nm) in the aqueous solutions if ion clustering did not occur but very close to the four closest anion distances (4.0 Å) in the KSCN crystal. The result suggests that the ions inside of the clusters have direct contact with each other.

4. CONCLUDING REMARKS

The results presented in the work demonstrate the potential of using vibrational energy transfers as a ruler to determine both static and transient intermolecular distances at the angstrom scale in both liquid and solid samples. The results also show that ions can form direct-contact ion clusters in relatively dilute strong electrolyte aqueous solutions. We expect that the studies of many fundamental problems in various fields will benefit from applying the vibrational energy transfer method, for example, the prenucleation of ions or molecules during the growth of crystals and nanomaterials, the formations of minerals in nature and bioinorganic composites (shells and bones) in living creatures, and the ion/biomolecular interactions. To achieve the ultimate goal of an “angstrom molecular ruler”, many more studies on more delocalized systems with shorter D/A distances and various D/A energy mismatches are needed. Advances in laser and detection technology for the fingerprint frequency region below 1000 cm^{-1} are also highly desirable for more sophisticated molecular systems.

■ ASSOCIATED CONTENT

Supporting Information

Supporting figures and data about FTIR, 2D-IR measurements, detailed derivation of equations, and data analyses. This

material is available free of charge via the Internet at <http://pubs.acs.org>.

AUTHOR INFORMATION

Corresponding Author

*E-mail: junrong@rice.edu.

Author Contributions

[†]H.C. and X.W. contributed equally to the work.

Notes

The authors declare no competing financial interest.

ACKNOWLEDGMENTS

This material is based upon work supported by the Welch foundation under Award No. C-1752 and AFOSR Award No. FA9550-11-1-0070. J.Z. also thanks the David and Lucile Packard Foundation for a Packard fellowship. Insightful discussions with Profs. Robert, F. Curl, Anatoly B. Kolomeisky, David Jonas, Greg Angel, Qiang Shi, and Donghui Zhang are appreciated.

REFERENCES

- (1) Förster, T. Zwischenmolekulare Energiewanderung Und Fluoreszenz. *Ann. Phys.* **1948**, *437*, 55–75.
- (2) Scholes, G. D. Long-Range Resonance Energy Transfer in Molecular Systems. *Annu. Rev. Phys. Chem.* **2003**, *54*, 57–87.
- (3) Bian, H. T.; Li, J. B.; Wen, X. W.; Zheng, J. R. Mode-Specific Intermolecular Vibrational Energy Transfer. I. Phenyl Selenocyanate and Deuterated Chloroform Mixture. *J. Chem. Phys.* **2010**, *132*, 184505.
- (4) Bian, H. T.; Wen, X. W.; Li, J. B.; Chen, H. L.; Han, S. Z.; Sun, X. Q.; Song, J. A.; Zhuang, W.; Zheng, J. R. Ion Clustering in Aqueous Solutions Probed with Vibrational Energy Transfer. *Proc. Natl. Acad. Sci. U.S.A.* **2011**, *108*, 4737–4742.
- (5) Bian, H.; Chen, H.; Li, J.; Wen, X.; Zheng, J. Nonresonant and Resonant Mode-Specific Intermolecular Vibrational Energy Transfers in Electrolyte Aqueous Solutions. *J. Phys. Chem. A* **2011**, *115*, 11657–11664.
- (6) Woutersen, S.; Bakker, H. J. Resonant Intermolecular Transfer of Vibrational Energy in Liquid Water. *Nature* **1999**, *402*, 507–509.
- (7) Akers, C.; Peterson, S. W.; Willett, R. D. A Refinement of Crystal Structure of KSCN. *Acta Crystallogr., Sect. B* **1968**, *24*, 1125–1126.
- (8) Cookson, D.; Finlayson, T.; Elcombe, M. Phonon Dispersion Relations for Potassium Thiocyanate. *Solid State Commun.* **1987**, *64*, 357–359.
- (9) Cookson, D.; Elcombe, M.; Finlayson, T. Phonon Dispersion Relations for Potassium Thiocyanate at and above Room Temperature. *J. Phys.: Condens. Matter* **1992**, *4*, 7851–7864.
- (10) Nagy, S. *Radiochemistry and Nuclear Chemistry*; Eolss Publishers Company Limited: Oxford, U.K., 2009.
- (11) Lakowicz, J. *Principles of Fluorescence Spectroscopy*, 3rd ed.; Springer: New York, 2006.
- (12) Kinosita, K.; Kawato, S.; Ikegami, A. A Theory of Fluorescence Polarization Decay in Membranes. *Biophys. J.* **1977**, *20*, 289–305.
- (13) Lipari, G.; Szabo, A. Effect of Librational Motion on Fluorescence Depolarization and Nuclear Magnetic Resonance Relaxation in Macromolecules and Membranes. *Biophys. J.* **1980**, *30*, 489–506.
- (14) Curl, R. F.; Kasper, J. V. V.; Pitzer, K. S. Nuclear Spin State Equilibration through Nonmagnetic Collisions. *J. Chem. Phys.* **1967**, *46*, 3220–3228.
- (15) Dale, R. E.; Eisinger, J.; Blumberg, W. The Orientational Freedom of Molecular Probes. The Orientation Factor in Intramolecular Energy Transfer. *Biophys. J.* **1979**, *26*, 161–193.
- (16) Savoie, R.; Tremblay, J. Raman Spectra of Crystals Immersed in Liquids. *J. Opt. Soc. Am.* **1967**, *57*, 329–332.
- (17) Chang, J. C. Monopole Effects on Electronic Excitation Interactions between Large Molecules. I. Application to Energy Transfer in Chlorophylls. *J. Chem. Phys.* **1977**, *67*, 3901–3909.